Effect of surfactants on single-bubble sonoluminescence

Kyuichi Yasui
Department of Physics, Waseda University, 3-4-1 Ohkubo, Shinjuku, Tokyo, Japan
(Received 2 April 1998)

The effect of surfactants on single-bubble sonoluminescence (SBSL) is studied theoretically based on the hot-spot model that a SBSL bubble collapses quasiadiabatically and that the quasi-thermal radiation is the origin of the light emission. Stottlemyer and Apfel [J. Acoust. Soc. Am. **102**, 1418 (1997)] reported that the surfactant called Triton X-100, which provides free interfacial motion, reduced the magnitude of the light pulse from the bubble. It is clarified by the present study that the effect of the surfactant is caused by the inhibition of condensation of water vapor at the bubble wall at the collapse, which results in lowering the achieved temperature inside a bubble due to the enhancement of the amount of vapor that undergoes endothermal chemical reactions. It is predicted, based on the hot-spot model, that the radiation is not thermalized inside a bubble in the case of SBSL in a solution of the surfactant in water and that the spectrum of SBSL may deviate from the blackbody spectrum and may have some characteristic lines such as the OH line (310 nm). It is suggested that surfactants can be used to enhance the chemical reactions of vapor in sonochemistry. It is also suggested that some of the surfactants are dissociated by the extremely high temperature at the bubble wall at the collapse. [S1063-651X(98)06610-0]

PACS number(s): 78.60.Mq

I. INTRODUCTION

In 1990, Gaitan [1] first reported the experiments of single-bubble sonoluminescence (SBSL). SBSL is a light emission phenomenon from a stably oscillating bubble in liquid irradiated by an ultrasonic wave [2]. The light is emitted at the collapse of the bubble. The pulse width of the light is experimentally measured to range from under 40 ps to over 350 ps [3–5]. The spectrum is broadband and can be fitted by the blackbody formula with the effective temperatures ranging from 6000 to 50 000 K [6–8]. The light pulse is emitted periodically with the frequency of the ultrasonic wave [3].

Recently, Stottlemyer and Apfel [9] reported the experiments of SBSL in solutions of surfactants in water. They reported that the surfactant called Triton X-100, which provides free interfacial motion, reduced the magnitude of the light pulse from the bubble [9]. It was also reported that the protein bovine serum albumin (BSA), which hinders interfacial motion, allowed the bubble to be driven to higher acoustic pressures, and resulted in an increase in the magnitude of the light pulse from the bubble [9].

With the addition of surfactants to water, a bubble is coated by the surfactants and the following effects are brought about: increase of the resistance of mass transfer at the bubble interface [10,11], change of the bulk viscosity of the liquid and the appearance of the surface viscosity [12–14], and the change of the surface tension [15,16]. In the present study of the effect of Triton X-100 on SBSL, only its effect on mass transfer is studied because the other effects are negligible on the large amplitude forced oscillations of a bubble in this case [16,17]. In the study of the effect of BSA, the effect of the surface viscosity and that of the enhanced surface tension by the addition of BSA in water are qualitatively discussed.

As discussed in other papers by the author [18,19], one of the promising models of SBSL is the hot-spot model that a collapse of a SBSL bubble is quasiadiabatic and that the quasithermal radiation is the origin of SBSL. Lohse, Brenner, Dupont, Hilgenfeldt, and Johnston [20] have clarified that a SBSL bubble in water containing air consists mainly of argon by the analysis of the experimental results concerning mass diffusion of a SBSL bubble. Thus in the present study, computer simulations of the oscillations of an argon bubble are performed, taking into account the effect of surfactants on evaporation or condensation of water at the bubble wall, based on the hot-spot model that includes the effect of thermal conduction both inside and outside a bubble, and that of chemical reactions inside a bubble.

II. MODEL

The model used in the present computer simulations is that of Ref. [18] for a SBSL bubble in pure water. For a SBSL in a solution of surfactants in water, one modification is made: the rate of evaporation and condensation of water vapor at the bubble wall [Eq. (7)]. The following is a brief description of the model.

The physical situation is that of a single spherical bubble in pure water or in a solution of surfactants in water, irradiated by an ultrasonic wave. An argon bubble is investigated, which consists of argon, water vapor, and small amounts of chemical products. Pressure (p_g) inside a bubble is assumed to be spatially uniform. The temperature inside a bubble is assumed to be spatially uniform except at the thermal boundary layer near the bubble wall. The width of the thermal boundary layer is assumed to be $n\lambda$ where n is a constant and λ is the mean free path of a gas molecule [21]. In the present calculation, $n=7$ is assumed [21].

In the model [18], the following effects are taken into account: thermal conduction both inside and outside the bubble, nonequilibrium evaporation and condensation of water vapor at the bubble wall, and chemical reactions inside the bubble. For a solution of surfactants in water, the effect

of surfactants on evaporation or condensation at the bubble wall is also taken into account as described later.

The equilibrium of the gas diffusion into and out of a bubble determines the ambient bubble radius (R_0) [17]. In the present computer simulations, the gas diffusion is neglected because it is a slow process compared to the bubble oscillations [17], whereas the ambient bubble radius (R_0) is determined by fitting the calculated results of radius-time curves with the experimental data reported by Stottlemyer and Apfel [9].

As the equation of bubble radius (R), Eq. (1) is employed, in which the compressibility of liquid and the effect of evaporation and condensation of water vapor at the bubble wall are taken into account [the derivation of Eq. (1) is given in Ref. [22]]:

$$\left(1-\frac{\dot R}{c_\infty}+\frac{\dot m}{c_\infty\rho_{L,i}}\right)R\ddot R+\frac{3}{2}\dot R^2\left(1-\frac{\dot R}{3c_\infty}+\frac{2\dot m}{3c_\infty\rho_{L,i}}\right)$$
$$=\frac{1}{\rho_{L,\infty}}\left(1+\frac{\dot R}{c_\infty}\right)\left[p_B-p_s\left(t+\frac{R}{c_\infty}\right)-p_\infty\right]$$
$$+\frac{\ddot m R}{\rho_{L,i}}\left(1-\frac{\dot R}{c_\infty}+\frac{\dot m}{c_\infty\rho_{L,i}}\right)$$
$$+\frac{\dot m}{\rho_{L,i}}\left(\dot R+\frac{\dot m}{2\rho_{L,i}}+\frac{\dot m\dot R}{2c_\infty\rho_{L,i}}-\frac{R}{\rho_{L,i}}\frac{d\rho_{L,i}}{dt}\right.$$
$$\left.-\frac{\dot m R}{c_\infty\rho_{L,i}^2}\frac{d\rho_{L,i}}{dt}\right)+\frac{R}{c_\infty\rho_{L,\infty}}\frac{dp_B}{dt}, \tag{1}$$

where the dot denotes the time derivative (d/dt), c_∞ is the sound speed in the liquid at infinity, $\dot m$ is the net rate of evaporation per unit area and unit time, $\rho_{L,i}(\rho_{L,\infty})$ is the liquid density at the bubble wall (at infinity), $p_B(t)$ is the liquid pressure on the external side of the bubble wall, $p_s(t)$ is a nonconstant ambient pressure component such as a sound field, and p_∞ is the undisturbed pressure. $p_B(t)$ is related to the pressure inside the bubble $[p_g(t)]$ by Eq. (2) [22,23],

$$p_B(t)=p_g(t)-\frac{2\sigma}{R}-\frac{4\mu}{R}\left(\dot R-\frac{\dot m}{\rho_{L,i}}\right)$$
$$-\dot m^2\left(\frac{1}{\rho_{L,i}}-\frac{1}{\rho_g}\right), \tag{2}$$

where σ is the surface tension, μ is the liquid viscosity, and ρ_g is the density inside the bubble. When a bubble is irradiated by an acoustic wave the wavelength of which is much larger than the bubble radius, $p_s(t)=-p_a\sin\omega t$ where p_a is the pressure amplitude of the acoustic wave and ω is its angular frequency.

In order to calculate the pressure inside the bubble $[p_g(t)]$, the van der Waals equation of state is employed,

$$\left(p_g(t)+\frac{a}{v^2}\right)(v-b)=R_gT, \tag{3}$$

where a and b are the van der Waals constants, v is the molar volume, R_g is the gas constant, and T is the temperature inside the bubble.

The temperature inside the bubble (T) is calculated by solving Eq. (4),

$$E=\frac{n_{\rm Ar}}{N_A}C_{V,{\rm Ar}}T+\frac{n_{\rm H_2O}}{N_A}C_{V,{\rm H_2O}}T$$
$$+\frac{T}{N_A}\sum_\alpha n_\alpha C_{V,\alpha}-\left(\frac{n_t}{N_A}\right)^2\frac{a}{V}, \tag{4}$$

where E is the thermal energy of the bubble, $n_{\rm Ar}(n_{\rm H_2O})$ is the number of argon (vapor) molecules inside the bubble, N_A is the Avogadro number, $C_{V,{\rm Ar}}(C_{V,{\rm H_2O}})$ is the molar heat of argon (vapor) at constant volume, α denotes species of the chemical products such as OH, O_2, O_3, HO_2, H_2O_2, H_2, H, and O, the summation is for all the chemical products considered here, n_t is the total number of molecules inside the bubble, and V is the volume of the bubble. The molar heat is assumed as follows: for monoatomic gases such as Ar, H, and O, the molar heat is $\frac{3}{2}R_g$, for diatomic gases such as OH, O_2, and H_2, it is $\frac{5}{2}R_g$, for the other gases, it is $\frac{6}{2}R_g$ [24].

The change of the thermal energy of a bubble (ΔE) in time Δt is expressed by [18]

$$\Delta E(t)=-p_g(t)\Delta V(t)+4\pi R^2\frac{10^3N_A}{M_{\rm H_2O}}\dot m e_{\rm H_2O}\Delta t$$
$$+4\pi R^2\kappa\left.\frac{\partial T}{\partial r}\right|_{r=R}\Delta t$$
$$+\frac{4}{3}\pi R^3\Delta t\sum_\gamma(r_{\gamma b}-r_{\gamma f})\Delta H_{\gamma f}+\left[-\frac{3}{5}M\dot R\ddot R\right]\Delta t, \tag{5}$$

where ΔV is the change of the bubble volume, $e_{\rm H_2O}$ is the energy carried by an evaporating or condensing vapor molecule, κ is the thermal conductivity of the gas inside a bubble, $\partial T/\partial r|_{r=R}$ is the temperature gradient at the bubble wall, $r_{\gamma f}(r_{\gamma b})$ is the forward (backward) reaction rate of the reaction γ per unit volume and unit time, $\Delta H_{\gamma f}$ is the enthalpy change in the forward reaction (when $\Delta H_{\gamma f}<0$, the reaction is exothermic), and M is the total mass of the gases inside the bubble. The first term on the right hand side of Eq. (5) is the work by the surrounding liquid (pV work). The second term is the energy carried by evaporating or condensing vapor molecules. The third term is the energy change due to thermal conduction. The fourth term is the heat of chemical reactions inside the bubble. The last term is the change of the kinetic energy of gases into heat. The brackets mean that this term is included only when the term is positive, which corresponds to the decrease of the kinetic energy. When the term is negative, it is replaced by zero.

In the model, the number of water molecules in the bubble ($n_{\rm H_2O}$) changes with time due to evaporation or condensation at the bubble wall and chemical reactions. For pure water, it is expressed by Eq. (6).

$$n_{H_2O}(t+\Delta t)=n_{H_2O}(t)+4\pi R^2\,\frac{10^3 N_A}{M_{H_2O}}\,\dot{m}\Delta t + \frac{4}{3}\,\pi R^3\Delta t[\Sigma(\text{production}) - \Sigma(\text{destruction})]. \quad (6)$$

The first sum in the right hand side of Eq. (6) contains the contribution of all reactions producing H_2O, and the second one contains that of all the reactions consuming H_2O. Details of the chemical kinetics are described in Refs. [18,19,25]. For a solution of surfactants in water, it is expressed by Eq. (7),

$$n_{H_2O}(t+\Delta t)=n_{H_2O}(t)+\left[4\pi(R^2-R_0^2)\,\frac{10^3 N_A}{M_{H_2O}}\,\dot{m}\Delta t\right] + \frac{4}{3}\,\pi R^3\Delta t[\Sigma(\text{production}) - \Sigma(\text{destruction})], \quad (7)$$

where R_0 is the ambient bubble radius, and $[\cdots]$ means that the term is included only when $R \geqslant R_0$, otherwise it is replaced by zero. The meaning of the term in the brackets $[\cdots]$ is that the bubble is completely coated by surfactants when the bubble radius is less than the ambient one (R_0) and that the fraction of the bubble surface coated by the surfactants completely inhibits evaporation and condensation of water vapor, assuming that the coated area is a constant ($4\pi R_0^2$) during the bubble oscillations due to the slowness of the diffusion of surfactants compared to the bubble oscillations. This picture of the reduction of evaporation or condensation at the bubble wall by surfactants is a crude one but is at least qualitatively accepted [11]. The rate of evaporation per unit area and unit time in the case of pure water ($\dot{m}$) is calculated by the formula described in Ref. [18].

In the model, the thermal conduction outside a bubble is taken into account and the liquid temperature at the bubble wall ($T_{L,i}$) varies with time [18,22]. Physical quantities of the liquid at the bubble wall are all calculated as functions of liquid temperature ($T_{L,i}$) [22]; density, saturated vapor pressure, thermal conductivity, latent heat of evaporation, viscosity, and surface tension. Their formulas are all described in Ref. [22].

III. RESULTS

Stottlemyer and Apfel [9] measured the bubble radius as a function of time from the images of a bubble captured with a microscope and a video camera. They reported the radius-time curves for three cases; (A) a SBSL bubble in pure water driven by the acoustic wave of which the frequency (f_a) and the amplitude (p_a) are 16.8 kHz and 1.25 atm, respectively, (B) a SBSL bubble in a solution of 0.1 critical micelle concentration (CMC) Triton X-100 in water with $f_a=16.4$ kHz and $p_a=1.26$ atm, and (C) a SBSL bubble in a solution of 1.0 CMC BSA in water with $f_a=16.3$ kHz and $p_a=1.327$ atm [9]. However, the resolution of the bubble images below a radius of about 5 μm is low and the measured values of the bubble radius at the bounces after the strongest collapse cannot be used to determine the ambient radius (R_0) which is a fitting parameter in the present calculations. Thus, in the present study, the maximum bubble radius (R_{max}) and the maximum radius after the first rebound (second R_{max}) are used to determine the ambient bubble radius (R_0).

TABLE I. The experimental data [9] and the calculated results of the maximum bubble radius (R_{max}) and the maximum bubble radius after the first rebound (second R_{max}) for the case of SBSL in pure water. p_a is the amplitude of the acoustic wave, and R_0 is the ambient bubble radius.

		Theory		
	Experiment [9]	$p_a=1.25$ atm $R_0=3$ μm	1.25 atm 8 μm	1.3 atm 5.5 μm
R_{max}	65 μm	43 μm	65 μm	65 μm
Second R_{max}	15 μm	10 μm	19 μm	16 μm

The calculations are performed for the above three cases [(A)–(C)]. For all the cases, the ambient liquid temperature (T_∞) and pressure (p_∞) are assumed to be 20 °C and 1 atm, respectively.

A. Pure water

In Table I the experimental data [9] and the calculated results of R_{max} and the second R_{max} are listed for the case of SBSL in pure water. It is seen that at the acoustic drive level of 1.25 atm, which is the experimentally reported value [9], the calculated results deviate significantly from the experimental data for any value of R_0. When $R_0=8$ μm, the calculated value of R_{max} coincides with the experimental data, but the calculated value of the second R_{max} is considerably larger than the experimental data. As R_0 is decreased, the calculated value of the second R_{max} decreases and coincides with the experimental data at some value of R_0, but R_{max} also decreases and becomes substantially smaller than the experimental data. Thus it is impossible to reproduce the experimental result of the radius-time curve by the theoretical calculations using $p_a=1.25$ atm. The agreement between the experimental data and the calculated results is achieved using a little bit larger value of p_a (1.3 atm) as seen in Table I.

The calculated results for the case of SBSL in pure water using $p_a=1.3$ atm and $R_0=5.5$ μm are shown in Fig. 1 and Figs. 2(a)–2(d). In Fig. 1 the bubble radius (R) is shown as a function of time for one acoustic cycle (59.5 μs); the circles are the experimental data [9] and the line is the calculated result. It is seen that at first a bubble expands due to the negative acoustic pressure, followed by a strong collapse. After the collapse, small bounces are seen.

In Figs. 2(a)–2(d) the calculated results at around the minimum bubble radius are shown as functions of time for 2000 ps (0.002 μs). In Fig. 2(a), the bubble radius (R) is shown. In Fig. 2(b) the temperature inside a bubble is shown. It is seen that the temperature rises up to 16 500 K. In Fig. 2(c) the blackbody radiance is shown, which is calculated by the Stefan-Boltzmann law of radiation [18]. The half-width

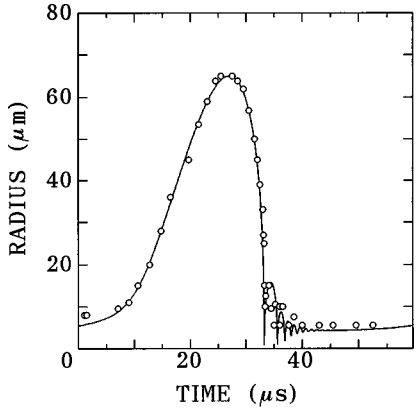

FIG. 1. The bubble radius as a function of time for one acoustic cycle (59.5 μs) for the case of SBSL in pure water with $p_a = 1.3$ atm and $R_0 = 5.5$ μm. The open circles are the experimental data [9] and the line is the calculated result.

of the blackbody radiance is 260 ps, which is consistent with the experimentally observed pulse width of SBSL [4,5].

Now we will discuss the condition of the thermalization of radiation inside a bubble. For the thermalization of radiation, the bubble radius must be larger than the mean free path of a photon (λ_{photon}). The mean free path of a photon is crudely estimated by $\lambda_{\text{photon}} = 1/\sigma_{bf} N_n$, where σ_{bf} is the cross section of photoionization of a highly excited atom and N_n is the number density of such highly excited atoms [19]. In Fig. 3 the size of the hot spot (R_h) necessary for the thermalization of radiation is shown as a function of temperature; above the line is the optically thick region where radiation is completely thermalized and below the line is the optically thin region where radiation is not thermalized. In the calculation of the line, $R_h = 5\lambda_{\text{photon}}$ is assumed as the criterion and the number density of molecules is assumed to be 10^{28} (m^{-3}) which is that when all the molecules undergo the van der Waals hard core collisions, and the number density of the highly excited molecules is assumed to be $N_n \sim qN$, where q is the degree of ionization calculated by the Saha equation [19]. More details of the thermalization of radiation are described in Ref. [19]. In Fig. 3 the solid circle is the calculated result for the case of SBSL in pure water and it is seen that the radiation is nearly thermalized inside a bubble.

In Fig. 2(d) the numbers of molecules inside a bubble are shown with the logarithmic vertical axis. It is seen that an appreciable amount of OH is created inside a bubble at the collapse.

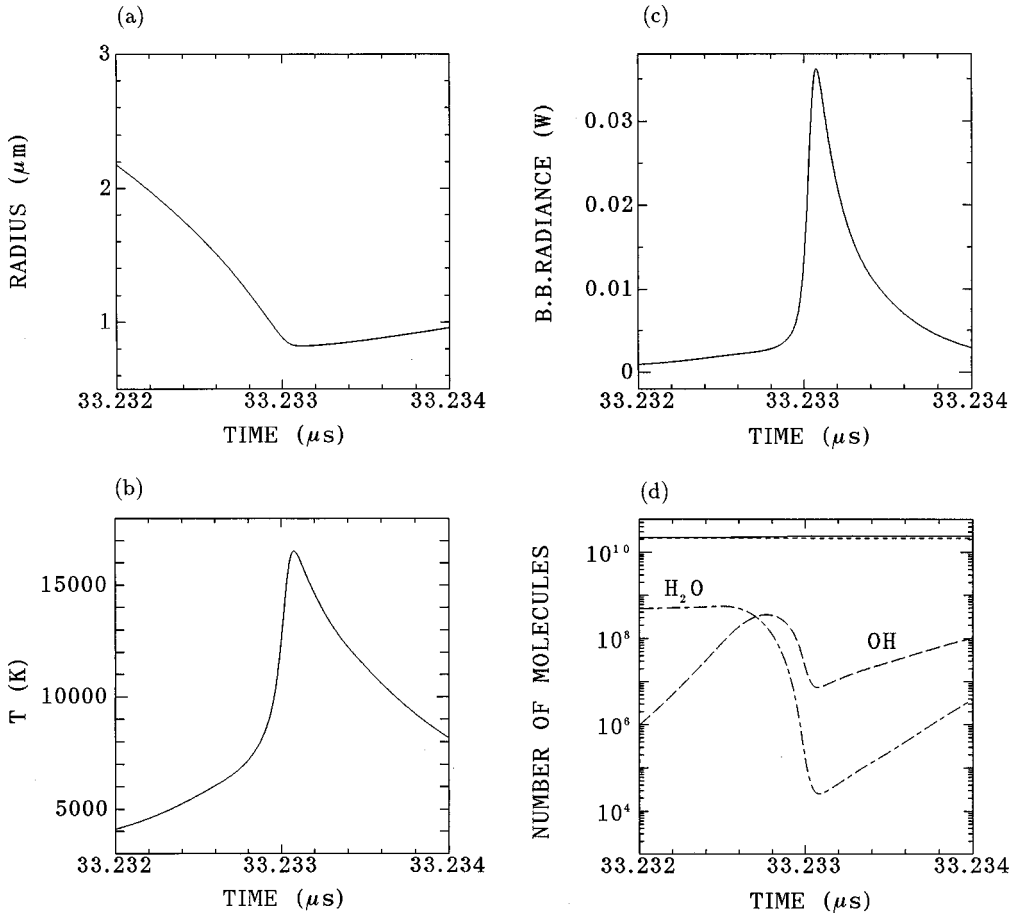

FIG. 2. Calculated results for the case of SBSL in pure water with $p_a = 1.3$ atm and $R_0 = 5.5$ μm at around the minimum bubble radius as functions of time for 2000 ps (0.002 μs). (a) The bubble radius (R). (b) The temperature inside the bubble (T). (c) The blackbody radiance. (d) The number of molecules inside the bubble with the logarithmic vertical axis. The solid line is the total number of molecules (n_t), the dotted line is the number of Ar molecules (n_{Ar}), the dash-dotted line is that of the H_2O molecules (n_{H_2O}), and the dotted line is that of the OH molecules.

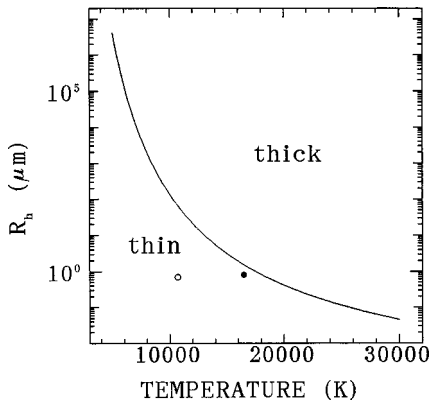

FIG. 3. Optically thick and thin regions in the phase space of the temperature and the radius of the hot spot (R_h). Above the line is the optically thick region and below the line is the optically thin region. The solid circle (the open circle) represents the calculated result for the case of SBSL in pure water (in a solution of 0.1 CMC Triton X-100 in water).

B. Triton X-100

In the case of SBSL in a solution of 0.1 CMC Triton X-100 in water, the best fitting parameters are $p_a = 1.3$ atm and $R_0 = 4.5$ μm. In Figs. 4(a)–4(c) and Figs. 5(a)–5(f) the calculated results are shown as functions of time. In Figs. 4(a)–4(c) physical quantities are shown for one acoustic cycle (61.0 μs). In Fig. 4(a) the bubble radius (R) is shown with the same vertical axis as that of Fig. 1(a); the circles are the experimental data [9] and the line is the calculated result. As in the case of SBSL in pure water, the calculated result of the radius-time curve fits well with the experimental data under the chosen parameters of p_a and R_0. In Fig. 4(b) the temperature inside a bubble (T) is shown with the logarithmic vertical axis. It is seen that the expansion of a bubble is isothermal while the collapse is quasiadiabatic as in the case of SBSL in pure water. In Fig. 4(c) the liquid temperature at the bubble wall ($T_{L,i}$) is shown with the same vertical axis as that of Fig. 4(b). It is seen that $T_{L,i}$ increases up to the same order of magnitude with the maximum temperature inside a bubble as in the case of SBSL in pure water. It is suggested that the surfactants at the bubble wall may be dissociated by the high temperature.

In Figs. 5(a)–5(f) the calculated results at around the minimum bubble radius are shown as functions of time for 2000 ps (0.002 μs). In Fig. 5(a) the bubble radius (R) is shown with the same vertical axis as that of Fig. 2(a). In Fig. 5(b) the temperature inside a bubble is shown with the same vertical axis as that of Fig. 2(b). It is seen that the maximum temperature inside a bubble (10 700 K) is much lower than that in the case of SBSL in pure water (16 500 K). As shown in Table II, if the effect of chemical reactions is completely neglected in the calculation, the result is the inverse; the maximum temperature inside a bubble in the case of SBSL in a solution of Triton X-100 in water is larger than that in the case of SBSL in pure water. Thus it is concluded that the lower maximum temperature in the case of Triton X-100 is caused by chemical reactions. In the case of Triton X-100, condensation of vapor at the collapse is inhibited by the surfactants at the bubble wall and many vapor molecules remain inside, which results in the increase of the amount of vapor

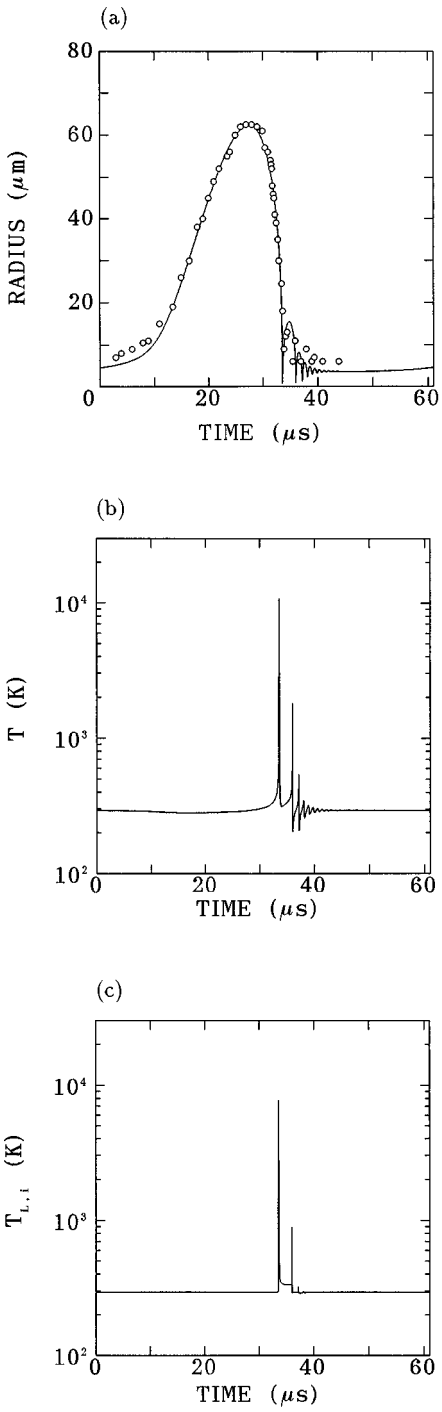

FIG. 4. Calculated results for the case of SBSL in a solution of 0.1 CMC Triton X-100 in water with $p_a = 1.3$ atm and $R_0 = 4.5$ μm as functions of time for one acoustic cycle (61.0 μs). (a) The bubble radius (R). The open circles are the experimental data [9] and the line is the calculated result. (b) The temperature inside the bubble (T). (c) The liquid temperature at the bubble wall ($T_{L,i}$).

undergoing chemical reactions as seen in Table III. Due to the endothermal nature of the chemical reactions, the maximum temperature inside a bubble in the case of Triton X-100 is lowered considerably, as seen in Table III.

In Table III, the changes of the physical quantities in the final 2000 ps (0.002 μs) of the collapse are listed. It is seen that the number of vapor molecules undergoing chemical

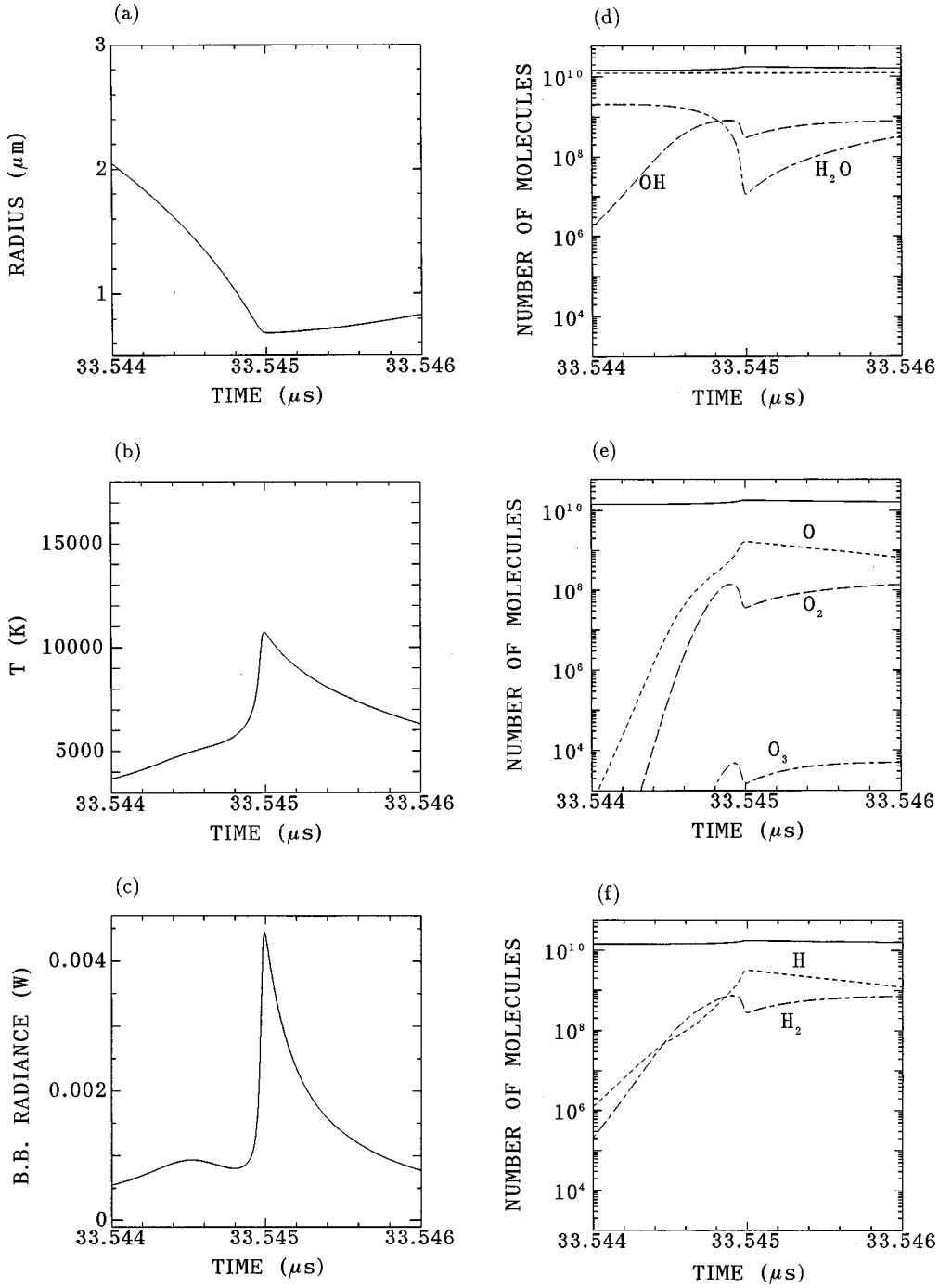

FIG. 5. Calculated results for the case of SBSL in a solution of 0.1 CMC Triton X-100 in water with $p_a = 1.3$ atm and $R_0 = 4.5$ μm at around the minimum bubble radius as functions of time for 2000 ps (0.002 μs). (a) The bubble radius (R). (b) The temperature inside the bubble (T). (c) The blackbody radiance. (d) The number of molecules inside the bubble with the logarithmic vertical axis. The solid line is the total number of molecules (n_t), the dotted line is the number of Ar molecules (n_{Ar}), the dash-dotted line is that of H_2O molecules ($n_{\mathrm{H_2O}}$), and the dotted line is that of OH molecules. (e) The number of O, O_2, and O_3 molecules inside the bubble. (f) The number of H and H_2 molecules inside the bubble.

reactions in the case of Triton X-100 is one order of magnitude larger than that in the case of pure water as mentioned above. The much lower maximum temperature in the case of Triton X-100 is due to the much smaller increase of the internal energy of a bubble in the final 2000 ps of the collapse. The main reason is the larger reduction of the internal energy by the endothermal chemical reactions in the case of Triton X-100, while the much smaller increase by pV work is also important.

It is concluded that the maximum temperature inside a bubble in the case of Triton X-100 is much smaller than that in the case of pure water, which is caused by the much larger amount of chemical reaction in the case of Triton X-100 due to the much larger amount of vapor remaining inside a

TABLE II. The calculated results at the minimum bubble radius including chemical reactions (CR) and those excluding CR. T is the temperature inside a bubble, E is the internal energy of a bubble, and n_t is the total number of molecules in a bubble.

	Pure water	0.1 CMC Triton X-100
R_0	5.5 μm	4.5 μm
p_a	1.3 atm	1.3 atm
T	16 100 K	10 600 K
(without CR)	(19 000 K)	(19 800 K)
E	7.9×10^{-9} J	3.9×10^{-9} J
(without CR)	$[9.0\times10^{-9}$ J]	$[6.7\times10^{-9}$ J]
n_t	2.4×10^{10}	1.8×10^{10}
(without CR)	(2.2×10^{10})	(1.4×10^{10})

bubble at the collapse by the inhibition of condensation at the bubble wall by the surfactants. It is suggested that surfactants may be used to increase the amount of chemical reaction of vapor inside a bubble in sonochemistry.

In Fig. 5(c) the blackbody radiance is shown. It should be noted that the scale of the vertical axis of Fig. 5(c) is about one order of magnitude less than that of Fig. 2(c), which is consistent with the experimental result that the intensity of SBSL in the case of Triton X-100 is much lower than that in the case of pure water [9]. However, as seen in Fig. 3, the radiation is not thermalized inside a bubble in this case. It is suggested that the spectrum of the light in this case may deviate significantly from the blackbody spectrum and that some characteristic lines such as the OH line (310 nm) may be seen. If such a spectrum is experimentally observed, the hot-spot model will be verified.

In Figs. 5(c)–5(f) numbers of molecules inside a bubble are shown with the same logarithmic vertical axes as that of Fig. 2(d). It is seen that much larger amounts of OH, O_2, O_3, H_2, HO_2, and H_2O_2 are created inside a bubble compared with those in the case of pure water, which is due to the much larger amount of vapor undergoing chemical reactions.

TABLE III. The change of the physical quantities in the final 2000 ps of the collapse. R is the bubble radius, T is the temperature inside a bubble, n_{H_2O} is the number of vapor molecules inside a bubble, ΔE is the change of the internal energy of a bubble in the final 2000 ps of the collapse. The contribution of each term in Eq. (5) to ΔE is also listed.

	Pure water	0.1 CMC Triton X-100
R	2.97–0.82 μm	2.83–0.68 μm
T	2900–16 100 K	2600–10 600 K
n_{H_2O}	5.6×10^{8}–2.8×10^{4}	2.1×10^{9}–1.2×10^{7}
ΔE	$+6.58\times10^{-9}$ J	$+3.06\times10^{-9}$ J
pV work	$+10.47\times10^{-9}$ J	$+6.29\times10^{-9}$ J
Thermal conduction	-3.86×10^{-9} J	-1.59×10^{-9} J
Change of kinetic energy	$+1.28\times10^{-9}$ J	$+1.10\times10^{-9}$ J
Heat of chemical reactions	-1.31×10^{-9} J	-2.74×10^{-9} J

TABLE IV. The experimental data [9] and the calculated results of the maximum bubble radius (R_{max}) and the maximum bubble radius after the first rebound (second R_{max}) for the case of SBSL in a solution of 1.0 CMC BSA in water. p_a is the amplitude of the acoustic wave, and R_0 is the ambient bubble radius.

		Theory	
	Experiment [9]	$p_a=1.33$ atm $R_0=4.5$ μm	1.38 atm 3 μm
R_{max}	68 μm	68 μm	70 μm
Second R_{max}	less than 10 μm	17 μm	21 μm

C. BSA

The protein bovine serum albumin hinders interfacial motion of a bubble by high surface viscosity and high surface tension [16]. In this case, it is impossible to reproduce the experimentally observed radius-time curve [9] by the theoretical calculations using any values of p_a and R_0. As seen in Table IV, the calculated second R_{max} is always much larger than the experimental data when the parameters (p_a and R_0) are chosen to reproduce the experimental data of R_{max}. Thus it is concluded that in the case of BSA the surface viscosity and the enhanced surface tension play an important role in bubble dynamics, which is not taken into account in the present calculations. For the discussion of the light emission in the case of BSA, these effects should be taken into account.

IV. CONCLUSION

The effect of surfactants on single-bubble sonoluminescence is studied theoretically based on the hot-spot model that a SBSL bubble collapses quasiadiabatically and that the quasi-thermal radiation is the origin of the light emission. It is clarified that the reduction of the magnitude of SBSL light by the addition of Triton X-100 [9] is due to the increase of the amount of endothermal chemical reactions, which results in the lower maximum temperature inside a bubble. The increase of the chemical reactions is due to the inhibition of condensation of vapor at the bubble wall by the surfactants, which results in the increase of the amount of vapor in a bubble at the final stage of the collapse when the chemical reactions take place. It is suggested that surfactants may be useful in increasing the amount of chemical reactions of vapor inside a bubble in sonochemistry. It is also suggested that some of the surfactants may be dissociated by the extremely high temperature at the bubble wall. It is predicted by the hot-spot model that in the case of SBSL in a solution of Triton X-100 in water the radiation inside a bubble is not thermalized and that the spectrum of the light may deviate significantly from the black-body spectrum and have some characteristic lines such as the OH line (310 nm). In order to study theoretically SBSL in a solution of BSA in water [9], the surface viscosity and the enhanced surface tension should be taken into account in the calculations of bubble dynamics.

[1] D. F. Gaitan, Ph.D. thesis, University of Mississippi, 1990; D. F. Gaitan, L. A. Crum, C. C. Church, and R. A. Roy, J. Acoust. Soc. Am. **91**, 3166 (1992).
[2] L. A. Crum, Phys. Today **47**(9), 22 (1994).
[3] B. P. Barber, R. Hiller, K. Arisaka, H. Fetterman, and S. Putterman, J. Acoust. Soc. Am. **91**, 3061 (1992).
[4] B. Gompf, R. Günther, G. Nick, R. Pecha, and W. Eisenmenger, Phys. Rev. Lett. **79**, 1405 (1997).
[5] R. Hiller, S. J. Putterman, and K. R. Weninger, Phys. Rev. Lett. **80**, 1090 (1998).
[6] R. Hiller, S. J. Putterman, and B. P. Barber, Phys. Rev. Lett. **69**, 1182 (1992).
[7] R. Hiller, Ph.D. thesis, University of California, 1995.
[8] D. F. Gaitan, A. A. Atchley, S. D. Lewia, J. T. Carlson, X. K. Maruyama, M. Moran, and D. Sweider, Phys. Rev. E **54**, 525 (1996).
[9] T. R. Stottlemyer and R. E. Apfel, J. Acoust. Soc. Am. **102**, 1418 (1997).
[10] M. M. Fyrillas and A. J. Szeri, J. Fluid Mech. **289**, 295 (1995).
[11] G. T. Barnes, Adv. Colloid Interface Sci. **25**, 89 (1986).
[12] G. N. Gottier, N. R. Amundson, and R. W. Flumerfelt, J. Colloid Interface Sci. **114**, 106 (1986).
[13] D. O. Johnson and K. J. Stebe, J. Colloid Interface Sci. **168**, 21 (1994).
[14] T. J. Asaki, D. B. Thiessen, and P. L. Marston, Phys. Rev. Lett. **75**, 2686 (1995).
[15] T. R. Stottlemyer, Ph.D. thesis, Yale University, 1996.
[16] R. G. Holt, Y. Tian, J. Jankovsky, and R. E. Apfel, J. Acoust. Soc. Am. **102**, 3802 (1997).
[17] T. G. Leighton, *The Acoustic Bubble* (Academic Press, London, 1994).
[18] K. Yasui, Phys. Rev. E **56**, 6750 (1997).
[19] K. Yasui (unpublished).
[20] D. Lohse, M. P. Brenner, T. F. Dupont, S. Hilgenfeldt, and B. Johnston, Phys. Rev. Lett. **78**, 1359 (1997).
[21] K. Yasui, J. Acoust. Soc. Am. **98**, 2772 (1995).
[22] K. Yasui, J. Phys. Soc. Jpn. **65**, 2830 (1996).
[23] S. Fujikawa and T. Akamatsu, J. Fluid Mech. **97**, 481 (1980).
[24] Y. S. Touloukian and T. Makita, *Specific Heat* (IFI/Plenum, New York, 1970).
[25] K. Yasui, J. Phys. Soc. Jpn. **66**, 2911 (1997).